JOURNAL OF Materials CHEMISTRY

Formation and characterization of Au–Ag bimetallic nanoparticles in water-in-oil microemulsions

Dong-Hwang Chen* and Cheng-Jia Chen

Department of Chemical Engineering, National Cheng Kung University, Tainan, Taiwan, 701, ROC. E-mail: chendh@mail.ncku.edu.tw; Fax: 886-6-2344496; Tel: 886-6-2757575 Ext.62680

Received 23rd November 2001, Accepted 11th February 2002
First published as an Advance Article on the web 20th March 2002

Gold–silver bimetallic nanoparticles with varying mole fractions were synthesized in water-in-oil microemulsions of water/Aerosol OT/isooctane by the co-reduction of $HAuCl_4$ and $AgNO_3$ with hydrazine at 25 °C. TEM analysis revealed that the bimetallic nanoparticles were essentially monodisperse and had a mean diameter of 4–22 nm, increasing with an increase in the molar ratio of water to Aerosol OT (ω_0) and Ag content. The UV/VIS absorption spectra of their solutions exhibited only one plasmon absorption and the absorption maximum of the plasmon band red-shifted almost linearly from 400 to 520 nm with increasing Au : Ag molar ratio, revealing the formation of an alloy. Although the characteristic peaks for Au and Ag were too close to distinguish, the XRD analysis showed that the characteristic peaks for a Au–Ag bimetallic systems became broader and accordingly suggested the formation of bimetallic nanoparticles. The EDX analysis confirmed directly the formation of Au–Ag bimetallic nanoparticles. It showed that the composition of Au–Ag bimetallic nanoparticles was in good agreement with that of the feed solution but the outer layer of the particles was enriched in Ag. The HRTEM study indicated the resultant Au–Ag bimetallic nanoparticles contained single and multiple twins as well as stacking faults, and no mismatch was present. In addition, it was found that the formation rate of Au nanoparticles was much faster than that of Ag nanoparticles. This satisfactorily accounted for the composition distribution within a Au–Ag bimetallic nanoparticle.

Introduction

In the past decade, considerable efforts have been devoted to bimetallic nanoparticles owing to their different catalytic properties,[1–3] surface plasma band energy,[4,5] and magnetic properties[6,7] relative to the individual metals. A number of methods have been used to prepare the bimetallic nanoparticles, including alcohol reduction,[1,8,9] citrate reduction,[5,10] polyol processes,[11] borohydride reduction,[12] solvent extraction–reduction,[4,13,14] sonochemical methods,[15] photolytic reduction,[16,17] radiolytic reduction,[18,19] laser ablation,[20,21] and metal evaporation–condensation.[22] The particle size was usually controlled *via* protective agents such as soluble polymers and organic ligands, or *via* the adsorption of anions on particle surface. It was shown that the size, structure, and composition distribution of the resultant particles depended on the preparation conditions.

Water-in-oil (w/o) microemulsions are transparent, isotropic, and thermodynamically stable with nano-sized water droplets that are dispersed in a continuous oil phase and stabilized by surfactant molecules at the water/oil interface. The surfactant-stabilized water pools provide a microenvironment for the preparation of nanoparticles by exchanging their contents *via* a fusion–redispersion process and preventing the excess aggregation of particles. As a result, the particles obtained in such a medium are generally very fine and monodisperse. Many kinds of nanoparticles have been prepared in w/o microemulsions including metals,[23–26] metal oxides and hydroxides,[27–30] metal sulfides and selenides,[31–35] metal borides,[36] metal carbonates,[37] organic polymers,[38] and so on. However, until recently when we synthesized Au–Pt, Au–Pd, and Pd–Pt bimetallic nanoparticles,[39–41] the preparation of bimetallic nanoparticles in w/o microemulsions had not been much attempted except for Cu–Au[42] and Pd–Pt.[43]

Au–Ag bimetallic nanoparticles receive significant attention because of their optical and electrochemical properties.[5,10,18] Their preparation has been achieved by citrate reduction,[5,10] borohydride reduction,[12] photolytic reduction,[17] radiolytic reduction,[18,19] laser ablation,[20] solvent extraction–reduction,[4,13] and evaporation–condensation.[22] Their preparation using microemulsion processing has not been reported. In this paper, the preparation of Au–Ag bimetallic nanoparticles in water-in-oil microemulsions of water/Aerosol OT/isooctane by the co-reduction of chloroauric acid and silver nitrate with hydrazine at 25 °C was studied. The size, optical properties, structure, and composition distribution of the resultant nanoparticles were characterized by transmission electron microscopy (TEM), UV/VIS spectroscopy, X-ray diffraction (XRD), high-resolution transmission electron microscopy (HRTEM), and energy dispersive X-ray analysis (EDX). The formation rates of particles were also investigated and the formation process was discussed.

Experimental

Silver nitrate and hydrazinium hydroxide were the guaranteed reagents of E. Merck (Darmstadt). Hydrogen tetrachloroaurate(III) hydrate was obtained from Alfa Aesar (Ward Hill, MA). Sodium bis(2-ethylhexyl) sulfosuccinate (Aerosol OT) purchased from Sigma Chemical Co. (St. Louis, MO) was vacuum dried at 60 °C for 24 h and stored in a vacuum desiccator before use. HPLC-grade isooctane supplied by TEDIA (Fairfield) was dehydrated with 4 Å molecular sieves (8–12 mesh, Janssen) for at least 24 h and kept in a vacuum desiccator prior to use. The residual water of the Aerosol OT/isooctane solution was recognized to be negligible by using a Karl-Fischer moisture titrator (Kyoto Electronics MKC-50). The water used throughout this work was the reagent-grade

water produced by the Milli-Q SP ultra-pure-water purification system from Nihon Millipore Ltd., Tokyo.

The w/o microemulsion solutions containing hydrazine, $HAuCl_4$ and $AgNO_3$ were prepared by injecting the required amount of the corresponding aqueous solution into an isooctane solution of Aerosol OT. The w/o microemulsion solutions containing both $HAuCl_4$ and $AgNO_3$ at a specified molar ratio were obtained by mixing the appropriate volumes of the w/o microemulsion solution containing $HAuCl_4$ and that containing $AgNO_3$.

The preparation of bimetallic and individual metallic nanoparticles was achieved by mixing equal volumes of two w/o microemulsion solutions at the same molar ratio of water to Aerosol OT (ω_0) and concentration of Aerosol OT, one containing an aqueous solution of metal salts and the other containing an aqueous solution of hydrazine. The reductions of $HAuCl_4$ and $AgNO_3$ were

$$4HAuCl_4 + 3N_2H_5OH \rightarrow 4Au + 16HCl + 3N_2 + 3H_2O \quad (1)$$

$$4AgNO_3 + N_2H_5OH \rightarrow 4Ag + 4HNO_3 + N_2 + H_2O \quad (2)$$

According to the findings of preliminary experiments, various nanoparticles usually reached their final sizes within several seconds to several tens of minutes, and so the samples for various analyses were taken after about 3 h. In this work the concentration of Aerosol OT was based on the overall volume of microemulsion solution, while the concentrations of metal salts and hydrazine were referred to the volume of aqueous solution added in the w/o microemulsion solution. In this study, the concentrations of Aerosol OT, hydrazine, and the total metal salts were fixed at 0.1 M, 1.0 M, and 0.1 M, respectively. The temperature was kept at 25 °C.

The particle sizes were determined by TEM using a JEOL Model JEM-1200EX at 80 kV. The sample for TEM analysis was obtained by placing a drop of the colloidal solution onto a Formvar-covered copper grid and evaporating it in air at room temperature. Before withdrawing the samples, the colloidal solutions were sonicated for 1 min to obtain better particle dispersion on the copper grid. For each sample, usually over 100 particles from different parts of the grid were used to estimate the mean diameter and size distribution of particles. The HRTEM study and EDX analysis were carried out on a Hitachi Model HF-2000 field emission transmission electron microscope with a resolution of 0.1 nm and the attached system. XRD measurements were performed on a Rigaku D/max III.V X-ray diffractometer using CuKα radiation (λ = 0.1542 nm). The UV/VIS spectra of the w/o microemulsion solutions containing various nanoparticles were measured with a Hitachi U-3000 spectrophotometer equipped with a 10 mm quartz cell. For the measurement of the formation rate of Au nanoparticles, the variation of absorbance at 520 nm with reaction time was observed in a stopped-flow spectrophotometer (Union Giken, RA401).

Results and discussion

The typical TEM micrographs and the size distributions of Au, Ag, and Au–Ag bimetallic nanoparticles at three different molar ratios obtained at ω_0 = 10 are shown in Fig. 1. Not only Au and Ag but also the Au–Ag bimetallic particles were very fine and essentially monodisperse. Since the difference in the mean diameter of Au (5 nm) and Ag (20 nm) was large enough to distinguish, the monodispersion of bimetallic systems suggested that they were not physical mixtures of the individual metallic nanoparticles and bimetallic nanoparticles were really formed.

The mean diameters of Au, Ag, and the bimetallic nanoparticles with various molar ratios of Au : Ag at ω_0 = 10 and 4 are illustrated in Fig. 2. As has been known, when the particle diameter reached that of the microemulsion droplet, the

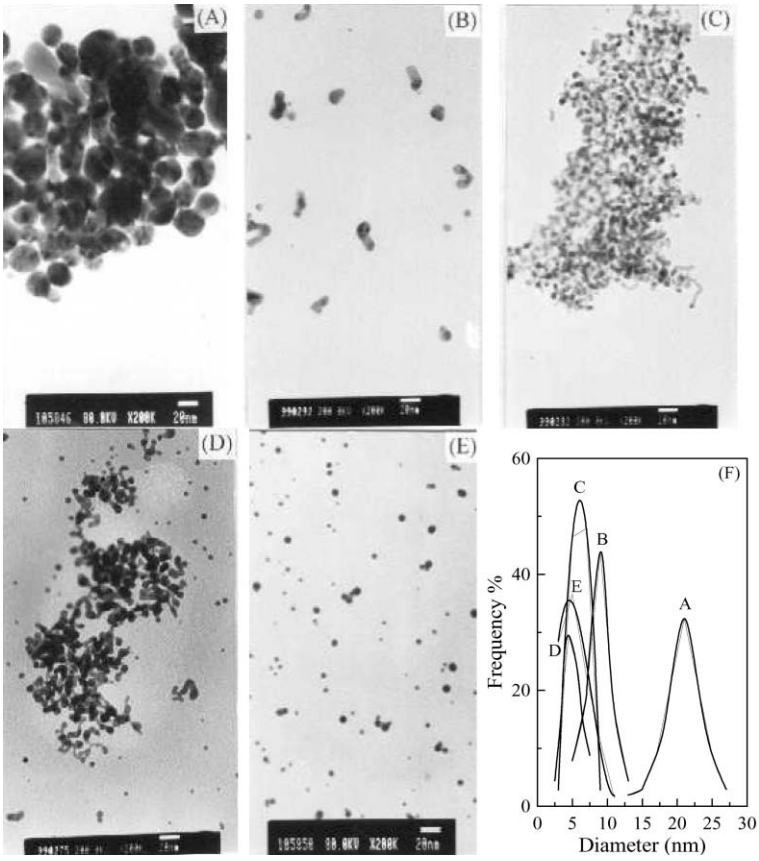

Fig. 1 Transmission electron micrographs and particle size distributions of the individual metallic and bimetallic nanoparticles: (A) Ag (B) Au–Ag (1 : 3) (C) Au–Ag (1 : 1) (D) Au–Ag (3 : 1) (E) Au. [metal salts] = 0.1 M; [N_2H_5OH] = 1.0 M; ω_0 = 10; AOT = 0.1 M; reaction time = 3 h (F) particle size distributions.

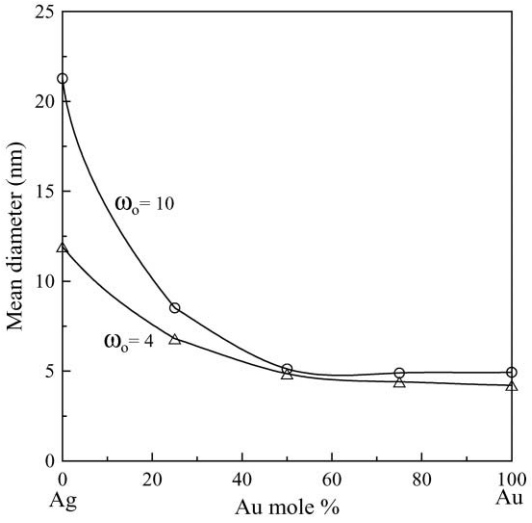

Fig. 2 Mean diameters of Au–Ag bimetallic nanoparticles as a function of composition in feed solution. [metal salts] = 0.1 M; [N_2H_5OH] = 1.0 M; [AOT] = 0.1 M; reaction time = 3 h.

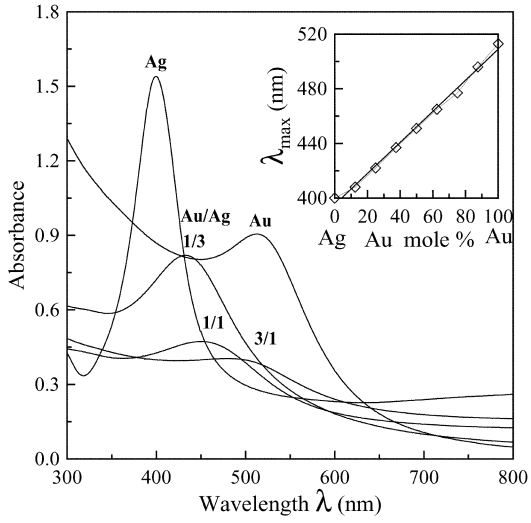

Fig. 3 UV/VIS absorption spectra of Au–Ag bimetallic nanoparticles at various molar ratios. The inset indicates the dependence of the absorption maximum of the plasmon band on the composition. [metal salts] = 0.1 M; [N_2H_5OH] = 1.0 M; ω_0 = 4; [AOT] = 0.1 M; reaction time = 3 h.

surfactant molecules might adsorb on the surface of the particle formed therein and restrict the growth of nanoparticles. The ω_0 value is a size-determining key parameter of microemulsion droplets and hence has an important influence on the particle size. So, it was reasonable that smaller particles were obtained at a lower ω_0 value due to the reduction in the size of microemulsion droplets. Furthermore, on increasing the Au content, the mean diameters of bimetallic nanoparticles decreased rapidly and then approached a constant value when the mole fraction of Au was above 50%. The dependence of the size of bimetallic nanoparticles on composition has been reported by several researchers. Yonezawa and Toshima found that the mean diameters of the bimetallic nanoparticles depended on the compositions and showed a negative deviation for the Pd–Pt, Au–Pd, and Au–Pt systems prepared by alcohol reduction,[9] while a positive deviation was observed by Esumi *et al.* for the Pd–Pt system prepared by solvent extraction reduction.[13] In our recent work concerning the synthesis of bimetallic nanoparticles in water-in-oil microemulsions, a negative deviation for the Au–Pt[39] and Au–Pd[40] systems and a positive deviation for the Pd–Pt[41] system were also observed. Although these results were not completely consistent, they were all ascribed to a difference in the nucleation process, which could be affected by the kinds of materials, the reaction media, and the preparation conditions.

It is known that, in addition to the collision energy and the sticking coefficient, the rates of nucleation and growth were determined mainly by the probabilities of the collisions between several atoms, between one atom and a nucleus, and between two or more nuclei. The former kind of collision related to the nucleation and the latter two kinds of collision to the growth process. When the reduction rate was so large that most of the ions were reduced before the formation of nuclei, and the probability of the effective collision between one atom and a nucleus was much higher than those of the other two collisions, the size of the resultant particles would be monodisperse and determined by the number of the nuclei formed at the very beginning of the reaction. Thus, in this work, the reduction of $AuCl_4^-$ and Ag^+ ions might be so fast that they were reduced almost completely before the formation of nuclei and the sizes of the Au, Ag, and Au–Ag bimetallic nanoparticles obtained were determined by the number of nuclei formed from Au or Ag. Since the concentration of total metal ions was fixed, the significant reduction in size due to the addition of Au at a low Au content as shown in Fig. 2 implied that Au might act as the seeds for the formation of Au–Ag bimetallic nanoparticles. Further discussion is given in the later study on formation kinetics of particles.

It is known that Au and Ag nanoparticles have plasmon absorption bands at about 520 and 400 nm, respectively. So, two plasmon bands would be expected for a physical mixture of Au and Ag monometallic nanoparticles and the formation of a Au–Ag alloy could be deduced from the fact that the optical absorption spectrum shows only one plasmon band. Fig. 3 shows the UV/VIS absorption spectra for Au, Ag and three typical Au–Ag bimetallic systems. Only one plasmon band was observed for each bimetallic system and the plasmon maximum was red-shifted almost linearly from 400 to 520 nm with increasing Au content as shown in the inset in Fig. 3, revealing the formation of a Au–Ag alloy. However, it was also noticed that the absorbance of Au–Ag bimetallic nanoparticles decreased with increasing Au content and they all were lower than those for Au and Ag. This result was in agreement with the calculated spectra of Au–Ag alloy nanoparticles using the full Mie equations.[44] According to the suggestion of Mulvaney *et al.*,[18] one monolayer of Au should be sufficient to mask the Ag plasmon resonance band completely. So, the above phenomenon could be due to the fact that the increased Au content on the particle surface resulted in the damping of the underlying Ag surface plasmon band.

Fig. 4 shows the XRD patterns of Au, Ag, and Au–Ag bimetallic nanoparticles. It was found that the XRD patterns for Au–Ag bimetallic systems exhibited broader characteristic peaks than those for the individual monometallic nanoparticles although the characteristic peaks for Au and Ag were too close to distinguish. This implied that Au–Ag bimetallic nanoparticles were formed and they were poorly crystalline resulting from less ordered structures as usually observed for nanoparticles. In addition, four characteristic peaks for Au and Ag marked by their indices ((111), (200), (220), and (311)) revealed that the resultant bimetallic nanoparticles were in the face-centered cubic (fcc) structure.

Three typical electron diffraction patterns for the Au–Ag bimetallic nanoparticles are shown in Fig. 5, in which the radii of four main fringe patterns were all in the ratio of $\sqrt{3} : 2 : \sqrt{8} : \sqrt{11}$. They related to the (111), (200), (220), and (311) planes and confirmed the fcc structure of Au–Ag alloy nanoparticles.

The HRTEM study on three typical Au–Ag bimetallic nanoparticles, as shown in Fig. 6, indicated the presence of defect structures. The particles contained single and multiple twins as well as stacking faults as observed for most

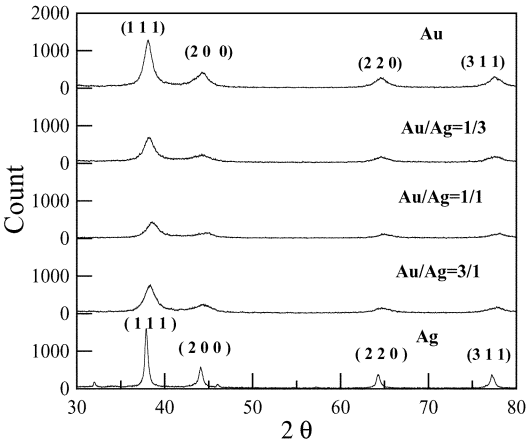

Fig. 4 XRD patterns of Au, Ag, and Au–Ag bimetallic nanoparticles at various molar ratios. [metal salts] = 0.1 M; $[N_2H_5OH]$ = 1.0 M; ω_0 = 4; [AOT] = 0.1 M; reaction time = 3 h.

nanoparticles, and the individual lattice planes were clearly visible. In addition, no mismatch was observed. This could be related to the very similar lattice constants of Au (0.408 nm) and Ag (0.4089 nm).[5]

For each molar ratio of Au : Ag, about 10 particles on the copper grid were chosen to analyze their average composition

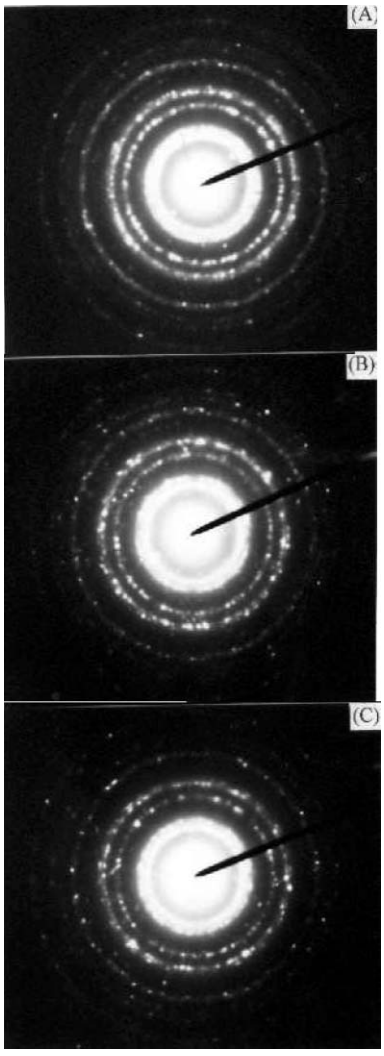

Fig. 5 Electron diffraction patterns of three typical Au–Ag bimetallic nanoparticles with various molar ratios. Au : Ag = 1 : 3 (A), 1 : 1 (B), 3 : 1 (C); [metal salts] = 0.1 M; $[N_2H_5OH]$ = 1.0 M; ω_0 = 4; [AOT] = 0.1 M; reaction time = 3 h.

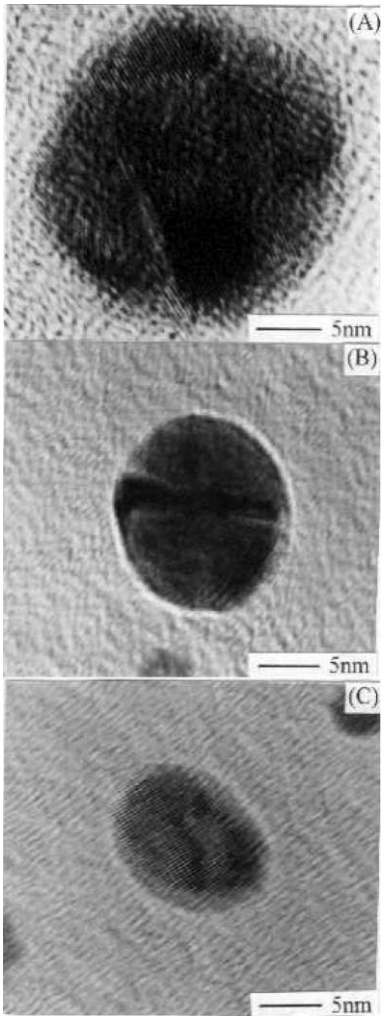

Fig. 6 High-resolution transmission electron microscopes of three typical Au–Ag bimetallic nanoparticles with various molar ratios. Au : Ag = 1 : 3 (A), 1 : 1 (B), 3 : 1 (C); [metal salts] = 0.1 M; $[N_2H_5OH]$ = 1.0 M; ω_0 = 10; [AOT] = 0.1 M; reaction time = 3 h.

by EDX. When the ratio of $[HAuCl_4]$: $[AgNO_3]$ in the feed solution was 1 : 3, 1 : 1, and 3 : 1, the Au : Ag elemental ratios of bimetallic nanoparticles were determined to be 24.63 : 75.37, 49.69 : 50.31, and 74.69 : 25.31, respectively. This revealed that the compositions of Au–Ag bimetallic nanoparticles were in good agreement with those of the two metal salts in the feed solutions, and confirmed directly the formation of Au–Ag bimetallic nanoparticles.

To further investigate the composition distribution within a particle, the compositions in the outer layer and in the core of a typical Au–Ag (1 : 3) nanoparticle were measured by EDX. It was found that the Au : Ag elemental ratios in the outer layer and in the core were 16.83 : 83.17 and 54.67 : 45.33, respectively. This indicated clearly that the outer layer of Au–Ag bimetallic nanoparticles was enriched in Ag. This might be related to the formation process and will be further discussed in the following section.

The formation rates of Au, Ag, and Au–Ag bimetallic nanoparticles were measured by observing the variations of their absorbance at the corresponding absorption maxima with time. In the case of Ag nanoparticles, the absorbance at 400 nm increased with time and then approached a constant value as shown in Fig. 7(A), revealing that the formation of Ag nanoparticles was completed in 30 min. For the preparation of Au nanoparticles, it was found that the color of the reaction solution turned instantaneously from yellow to red. Since the formation rate was so quick that the required time could not be detected by conventional methods, a stopped-flow

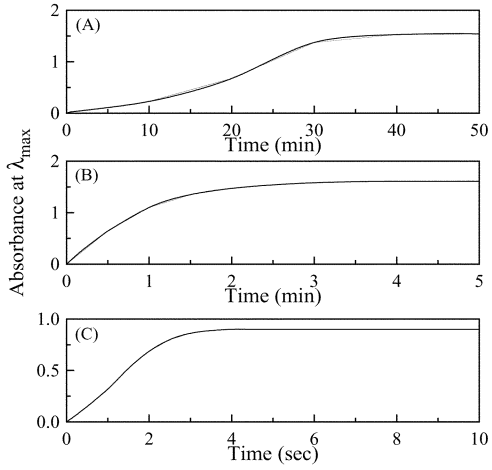

Fig. 7 Absorbance changes for metallic and bimetallic nanoparticles with reaction time at their corresponding absorption maxima. (A) Ag at 400 nm, (B) Au–Ag (1 : 3) at 429 nm, (C) Au at 520 nm; $[HAuCl_4]$ = 0.1 M; $[N_2H_5OH]$ = 1.0 M; ω_0 = 4; [AOT] = 0.1 M.

spectrophotometer was used to measure the formation rate of Au nanoparticles. As shown in Fig. 7(C), the time required for the complete formation of Au nanoparticles was only 4 s. In the case of Au–Ag (1 : 3), a similar tendency at 429 nm was observed but the time required for the formation of bimetallic nanoparticles was reduced to 3 min, as illustrated in Fig. 7(B). This indicated that the formation of bimetallic nanoparticles was significantly accelerated by the presence of Au, although it was still slower than that for Au. This could be attributed to the seeding effect of Au.

Thus, according to the above investigations on the effect of composition on particle size, the composition distribution in a particle, and the rates of particle formation, the formation process of Au–Ag bimetallic nanoparticles could be described as follows. First, $AuCl_4^-$ and Ag^+ ions are reduced completely. Then, Au and Ag atoms start to aggregate to form the nuclei. Since the nucleation rate of Au is much faster than that of Ag, the nuclei of the bimetallic system might be formed mainly from Au atoms. All nuclei might be formed almost at the same time. After that, the bimetallic nanoparticles grow gradually to their final size by the co-deposition of Au and Ag atoms on the nuclei. Au atoms should be more likely to deposit on the nuclei. This leads to the enrichment of Ag in the outer layer of Au–Ag bimetallic nanoparticles.

Conclusions

Au–Ag bimetallic nanoparticles have been prepared in microemulsions of water/AOT/isooctane by the co-reduction of $HAuCl_4$ and $AgNO_3$ with hydrazine. The particle size analysis indicated that the resultant bimetallic nanoparticles were monodisperse and had a mean diameter of 4–22 nm, increasing with an increase in the ω_0 ($[H_2O]/[AOT]$) value and Ag content. The rapid reduction in particle size due to the addition of a small amount of Au suggested that Au might play a seeding role in the formation of Au–Ag bimetallic nanoparticles. Both the UV/VIS absorption spectra and XRD patterns for the bimetallic systems revealed the formation of bimetallic nanoparticles. The HRTEM study indicated the particles contained single and multiple twins as well as stacking faults, and no mismatch was present. The EDX analysis confirmed directly the formation of bimetallic nanoparticles and showed that Ag atoms were enriched in the outer layer of bimetallic nanoparticles. In addition, the formation rate of Au nanoparticles was found to be much faster than that of Ag nanoparticles. Also, Au might act as the seeds for the formation of Au–Ag bimetallic nanoparticles. According to the kinetic analysis and the characterization of particles, a formation process for Au–Ag bimetallic nanoparticles was proposed. This work showed another practicable method for the preparation of Au–Ag bimetallic nanoparticles, and should be helpful for the clarification of the formation process of Au–Ag bimetallic nanoparticles in w/o microemulsions.

Acknowledgement

This work was performed under the auspices of the National Science Council of the Republic of China, under contract number NSC 89-2214-E006-034, to which the authors wish to express their thanks.

References

1 N. Toshima, T. Yonezawa and K. Kushihashi, *J. Chem. Soc., Faraday Trans.*, 1993, **89**, 2537.
2 M. Harada, K. Asakura, Y. Ueki and N. Toshima, *J. Phys. Chem.*, 1993, **97**, 5103.
3 Y. Wang and N. Toshima, *J. Phys. Chem. B*, 1997, **101**, 5301.
4 S. W. Han, Y. Kim and K. Kim, *J. Colloid Interface Sci.*, 1998, **208**, 272.
5 S. Link, S. Z. L. Wang and M. A. El-Sayed, *J. Phys. Chem. B*, 1999, **103**, 3529.
6 B. Bian, Y. Hirotsu, K. Sato, T. Ohkubo and A. Makino, *J. Electron Microsc.*, 1999, **48**, 753.
7 S. Sun, C. B. Murry, D. Weller, L. Folks and A. Moser, *Science*, 2000, **287**, 1989.
8 N. Toshima and Y. Wang, *Langmuir*, 1994, **10**, 4574.
9 T. Yonezawa and N. Toshima, *J. Chem. Soc., Faraday Trans.*, 1995, **91**, 4111.
10 R. G. Freeman, M. B. Hommer, K. C. Grabar, M. A. Jackson and M. J. Natan, *J. Phys. Chem.*, 1996, **100**, 718.
11 P.-Y. Silvert, V. Vijayakrishnan, P. Vibert, R. Herrera-Urbina and K. T. Elhsissen, *Nanostruct. Mater.*, 1996, **7**, 611.
12 L. M. Liz-Marzán and A. P. Philipse, *J. Phys. Chem.*, 1995, **99**, 15120.
13 K. Esumi, M. Shiratori, H. Ishizuka, T. Tano, K. Torigoe and K. Meguro, *Langmuir*, 1991, **7**, 457.
14 M. Brust, M. Walker, D. Bethell, D. J. Schiffrin and R. Whyman, *J. Chem. Soc., Chem. Commun.*, 1994, 801.
15 Y. Mizukoshi, K. Okitsu, Y. Maeda, T. A. Yamamoto, R. Oshima and Y. Nagata, *J. Phys. Chem. B*, 1997, **101**, 7033.
16 S. Remita, M. Mostafavi and M. O. Delcourt, *Radiat. Phys. Chem.*, 1996, **47**, 275.
17 T. Sato, S. Kuroda, A. Takami, Y. Yonezawa and H. Hada, *Appl. Organomet. Chem.*, 1991, **5**, 261.
18 P. Mulvaney, M. Giersig and A. Henglein, *J. Phys. Chem.*, 1993, **97**, 7061.
19 M. Treguer, C. de Cointet, H. Remita, J. Khatouri, M. Mostafavi, J. Amblard, J. Belloni and R. de Keyzer, *J. Phys. Chem. B*, 1998, **102**, 4310.
20 J. H. Hodak, A. Henglein, M. Giersig and G. V. Hartland, *J. Phys. Chem. B*, 2000, **104**, 11708.
21 Y. H. Chen and C. S. Yeh, *Chem. Commun.*, 2000, 371.
22 G. C. Papavassiliou, *J. Phys. F: Met. Phys.*, 1976, **6**, L103.
23 M. Boutonnet, J. Kizling, P. Stenius and G. Maire, *Colloids Surf.*, 1982, **5**, 209.
24 C. Petit, P. Lixon and M. P. Pileni, *J. Phys. Chem.*, 1993, **97**, 12974.
25 I. Lisiecki and M. P. Pileni, *J. Am. Chem. Soc.*, 1993, **115**, 3887.
26 D. H. Chen and S. H. Wu, *Chem. Mater.*, 2000, **12**, 1354.
27 K. Osseo-Asare and F. Arriagada, *J. Colloid Interface Sci.*, 1990, **50**, 321.
28 V. Pillai, P. Kumar, M. S. Multani and D. O. Shah, *Colloid Surf. A*, 1993, **80**, 69.
29 E. Joselevich and I. Willner, *J. Phys. Chem.*, 1994, **98**, 7628.
30 C. L. Chang and H. S. Fogler, *Langmuir*, 1997, **13**, 3295.
31 P. Lianos and J. K. Thomas, *J. Colloid Interface Sci.*, 1987, **117**, 505.
32 R. Kortan, R. Hull, R. L. Opila, M. G. Bawendi, M. L. Steigerwald, P. J. Carroll and L. E. Brus, *J. Am. Chem. Soc.*, 1990, **112**, 1327.
33 J. Ward, E. C. O'Sullivan, J.-C. Rang, J. Nedeljkovic and R. C. Patel, *J. Colloid Interface Sci.*, 1993, **161**, 316.
34 S. K. Haram, A. R. Mahadeshwar and S. G. Dixit, *J. Phys. Chem.*, 1996, **100**, 5868.

35 M. P. Pileni, *Catal. Today*, 2000, **58**, 151.
36 J. Nagy, *J. Colloids Surf.*, 1989, **35**, 201.
37 K. Kandori, K. Kon-No and A. Kitahara, *J. Colloid Interface Sci.*, 1988, **122**, 78.
38 N. Moumen, M. P. Pileni and R. A. Mackay, *Colloid Surf. A.*, 1999, **151**, 409.
39 M. L. Wu, D. H. Chen and T. C. Huang, *Chem. Mater.*, 2001, **13**, 599.
40 M. L. Wu, D. H. Chen and T. C. Huang, *Langmuir*, 2001, **17**, 3877.
41 M. L. Wu, D. H. Chen and T. C. Huang, *J. Colloid Interface Sci.*, 2001, **243**, 102.
42 R. Touroude, P. Girard, G. Maire, J. Kizling, M. Boutonnet-Kizling and P. Stenius, *Colloid Surf.*, 1992, **67**, 9.
43 C. Sangregorio, M. Galeotti, U. Bardi and P. Baglioni, *Langmuir*, 1996, **12**, 5800.
44 P. Mulvaney, *Langmuir*, 1996, **12**, 788.